

## Reversibility of minor hysteresis loops in magnetocaloric Heusler alloys

Tino Gottschall, Enric Stern-Taulats, Lluís Mañosa, Antoni Planes, Konstantin P. Skokov, and Oliver Gutfleisch

Citation: *Appl. Phys. Lett.* **110**, 223904 (2017); doi: 10.1063/1.4984797

View online: <http://dx.doi.org/10.1063/1.4984797>

View Table of Contents: <http://aip.scitation.org/toc/apl/110/22>

Published by the [American Institute of Physics](#)

---

---



**FIND THE NEEDLE IN THE  
HIRING HAYSTACK**

POST JOBS AND REACH THOUSANDS OF  
QUALIFIED SCIENTISTS EACH MONTH.

PHYSICS TODAY | JOBS  
[WWW.PHYSICSTODAY.ORG/JOBS](http://WWW.PHYSICSTODAY.ORG/JOBS)

## Reversibility of minor hysteresis loops in magnetocaloric Heusler alloys

Tino Gottschall,<sup>1,a)</sup> Enric Stern-Taulats,<sup>2</sup> Lluís Mañosa,<sup>2</sup> Antoni Planes,<sup>2</sup>  
 Konstantin P. Skokov,<sup>1</sup> and Oliver Gutfleisch<sup>1</sup>

<sup>1</sup>Technische Universität Darmstadt, Institut für Materialwissenschaft, Alarich-Weiss-Str. 16,  
 64287 Darmstadt, Germany

<sup>2</sup>Departament de Física de la Matèria Condensada, Facultat de Física, Universitat de Barcelona,  
 Diagonal 647, 08028 Barcelona, Catalonia, Spain

(Received 1 March 2017; accepted 16 May 2017; published online 2 June 2017)

The unavoidable existence of thermal hysteresis in magnetocaloric materials with a first-order phase transition is one of the central problems limiting their implementation in cooling devices. Using minor loops, however, allows achieving significant cyclic effects even in materials with relatively large hysteresis. Here, we compare thermometric measurements of the adiabatic temperature change  $\Delta T_{\text{ad}}$  and calorimetric measurements of the isothermal entropy change  $\Delta S_T$  when moving in minor hysteresis loops driven by magnetic fields. Under cycling in 2 T, the Ni-Mn-In-Co Heusler material provides a reversible magnetocaloric effect of  $\Delta S_T^{\text{rev}} = 10.5 \text{ J kg}^{-1} \text{ K}^{-1}$  and  $\Delta T_{\text{ad}}^{\text{rev}} = 3.0 \text{ K}$ . Even though the thermodynamic conditions and time scales are very different in adiabatic and isothermal minor loops, it turns out that after a suitable scaling, a self-consistent reversibility region in the entropy diagram is found. This region is larger than expected from basic thermodynamic considerations based on isofield measurements alone, which opens new opportunities in application. Published by AIP Publishing. [<http://dx.doi.org/10.1063/1.4984797>]

Significant magnetocaloric effects can nowadays be obtained in many different materials in magnetic field changes of 1 to 2 T.<sup>1–3</sup> However, it depends on the reversible contribution whether those compounds can be implemented into cooling machines.<sup>4</sup> In materials undergoing a first-order transition, the occurrence of thermal hysteresis diminishes the reversibility of the transformation.<sup>5</sup> The reduction of the hysteresis is therefore a desirable goal.<sup>6</sup> For instance in Heusler-type compounds, narrowing the hysteresis width and retaining large magnetocaloric effects at the same time is an extremely challenging task.<sup>7</sup> Instead, in the so-called minor loops a certain hysteresis is tolerable and yet significant magnetocaloric effects under cycling can be achieved.<sup>8</sup> The aim of this paper is to deepen the understanding of the transformation processes in minor hysteresis loops in order to find strategies to enhance their efficiency further. These findings will bring Heusler alloys a step forward to their implementation in environmentally friendly cooling technologies.

For our experimental study, we selected the representative quaternary Heusler alloy  $\text{Ni}_{45.7}\text{Mn}_{36.6}\text{In}_{13.5}\text{Co}_{4.2}$  because of its outstanding magnetocaloric properties. The sample was prepared by arc melting from high purity elements and a subsequent heat treatment at 900° for 24 h followed by water quenching. Magnetic measurements were carried out using a commercial Quantum Design PPMS 14T system. For the thermometric and the calorimetric measurements, a block with the dimensions of  $6 \times 3 \times 2 \text{ mm}^3$  was cut from the heat-treated ingots. Before each experiment sequence, the material was heated to the pure austenite state and subsequently cooled to pure martensite in order to erase the memory of the transition.<sup>9</sup> The adiabatic temperature change  $\Delta T_{\text{ad}}$  was determined directly using a purpose-built device.<sup>10</sup> The sample temperature was measured by a thermocouple placed

inside the specimen. For the experimental determination of the entropy change  $\Delta S_T$ , a dedicated calorimeter was used.<sup>11</sup> Isofield calorimetric measurements in magnetic fields up to 5 T were performed with heating and cooling rates of  $0.6 \text{ K min}^{-1}$ . The procedure for the data treatment is described in Ref. 11. Isothermal calorimetric experiments were performed after stabilizing times of more than 90 min. The magnetic field sweeping rate was set to  $0.16 \text{ T min}^{-1}$ . In order to monitor minor hysteresis loops, the magnetic field of 2 T was ramped up and down twice.

Both the magnetization  $M$  and the calorimetric signal  $\frac{dQ}{dT}$  of the sample are shown as a function of temperature in various magnetic fields in Fig. 1(a). Despite the different heating and cooling rates during the measurements, the obtained result agrees quite well. Increasing the magnetic field leads to a shift of the transition to lower temperatures as can also be seen in the magnetic phase diagram shown in Fig. 1(b). Therefore, Ni-Mn-In-Co exhibits an inverse magnetocaloric effect. The calorimetric curves for heating and cooling in the upper part of Fig. 1(a) look very different. Under heating, basically only a single broad heat flow peak is visible, whereas the cooling of the sample results in a very spiky signal. Those spikes are due to the formation of martensite nuclei and their avalanche-like growth in the austenite matrix.<sup>12</sup> However, the backward transition into austenite takes place in a much smoother way.

Integrating the calorimetric curves over temperature allows us to determine the entropy change of the complete transition  $\Delta S_t$  but also the phase fraction of austenite and martensite as done for instance in Refs. 13 and 14. The respective  $\Delta S_t$  for heating and cooling is plotted in the bottom part of Fig. 1(b). It can be seen that the entropy change is reducing with increasing magnetic field. This reduction is due to the strengthening of the magnetic entropy part at lower temperatures competing with the structural contribution.<sup>15</sup>

<sup>a)</sup>gottschall@fm.tu-darmstadt.de

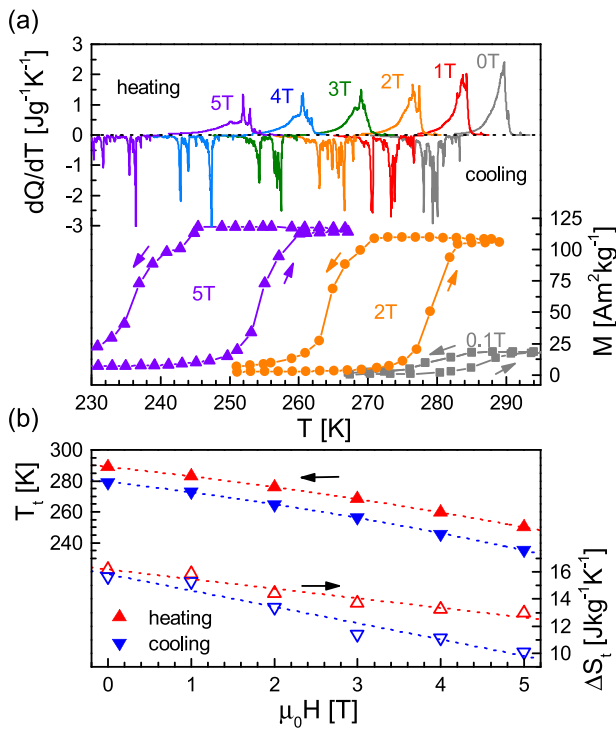


FIG. 1. (a) Calorimetric signal (upper part) and magnetization (lower part) as a function of temperature in different constant magnetic fields under heating and cooling. (b) Magnetic phase diagram and entropy change of the transition  $\Delta S_t$  in different magnetic fields obtained from calorimetric measurements.  $T_t$  corresponds to the middle point of the transition under heating and cooling.

Based on the calorimetric data and heat capacity measurements, it is possible to extract the  $S(T, H)$  diagram under heating and cooling.<sup>16</sup> The entropy curves are plotted as solid and dashed lines in Fig. 2 for zero field and 2 T, respectively. In addition, the field-induced magnetocaloric effect, namely the adiabatic temperature change  $\Delta T_{ad}$  and the isothermal entropy change  $\Delta S_T$  are plotted as horizontal and vertical arrows. The measurement of  $\Delta T_{ad}$  was performed in a rotating nested Halbach array providing a field change of 1.93 T using a maximum field rate of 42 T min<sup>-1</sup> (Ref. 17). Instead,  $\Delta S_T$  was obtained in the calorimeter being equipped with a superconducting magnet using a field rate of 0.16 T min<sup>-1</sup>. It should be highlighted that all those measurements were performed on the same specimen in order to allow a meaningful comparison. It can be seen in Fig. 2(a) that the different setups and experiments are in good agreement. The horizontal ( $\Delta T_{ad}$ ) and vertical arrows ( $\Delta S_T$ ) starting on the zero-field entropy curve under heating approach the 2 T curve as expected.<sup>18</sup>

Those arrows indicate the magnetocaloric effect of the first field application only. The reversibility was therefore studied in a second magnetic field sequence. The cyclic  $\Delta T_{ad}$  and  $\Delta S_T$  values are illustrated as horizontal and vertical bars in Fig. 2(b). From thermodynamics, one would expect that those bars reflect the enclosed area between the entropy curves in 2 T under heating (red dashed) and in zero-field under cooling (blue solid line).<sup>19</sup> However, our results clearly show that the reversibility area is in fact much larger. Especially around a temperature of 280 K and above where no cyclability of the first-order transition would be expected, a

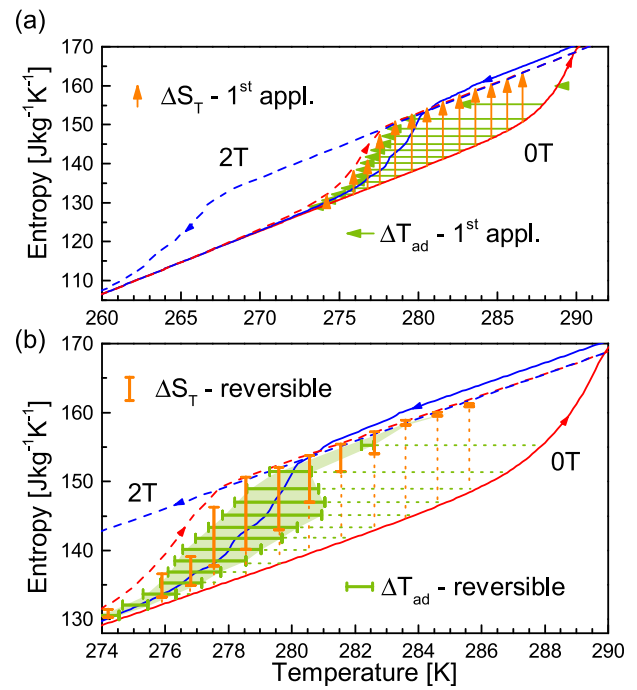


FIG. 2. (a) Entropy diagram of Ni<sub>45.7</sub>Mn<sub>36.6</sub>In<sub>13.5</sub>Co<sub>4.2</sub>. The red and blue lines indicate the  $S(T, H)$  curves in 0 T (solid lines) and 2 T (dashed lines) under heating and cooling. The green horizontal arrows illustrate the adiabatic temperature change of the first field application. The isothermal entropy change  $\Delta S_T$  is plotted as orange vertical arrows. (b) Magnified area of the  $S(T, H)$  diagram. The reversible  $\Delta S_T$  and  $\Delta T_{ad}$  are shown as orange and green bars spanning the highlighted reversibility area.

significant reversible magnetocaloric effect is evident in both adiabatic and isothermal experiments. This behavior is due to the special characteristics of minor loops of hysteresis and cannot be predicted from isofield measurements straightforwardly.<sup>8</sup> Thus, the optimal condition with the largest reversible isothermal entropy change of  $\Delta S_T^{\text{rev}} = 10.5 \text{ J kg}^{-1} \text{ K}^{-1}$  and adiabatic temperature change of  $\Delta T_{ad}^{\text{rev}} = 3.0 \text{ K}$  is situated around the mid-region with 50% martensite and austenite. This seems to be a general rule of thumb for minor loop processes, since similar results have been demonstrated for other Ni-Mn-based Heusler alloys without Cobalt.<sup>20</sup>

Figure 2 only represents a partial information of the transformation. In order to study the specific paths during the martensitic transition, we need to plot the  $S(T, H)$  diagram in three dimensions instead as shown in Fig. 3. The entropy curves under heating and cooling were measured in constant magnetic fields of 0, 1, and 2 T and are therefore lying parallel to the  $S$ - $T$ -plane. The transition region is, therefore, shifted along the diagonal of this plane since the transformation temperature is lowered in magnetic fields. Those 6 curves consequently span a volume in which the back and forth transition between martensite and austenite has to take place. In addition, the transformation paths when applying a magnetic field of 2 T under adiabatic conditions (at constant entropy in the  $T$ - $H$ -plane) and under isothermal conditions (at constant temperature in the  $S$ - $H$ -plane) are plotted as dotted lines. For instance, the isothermal experiment obtained at highest temperature of 286.6 K starts in the mostly martensitic state in zero field. After sweeping the magnetic field above 0.2 T, the transition is started and a steep increase of the entropy change is observed until the pure austenite state

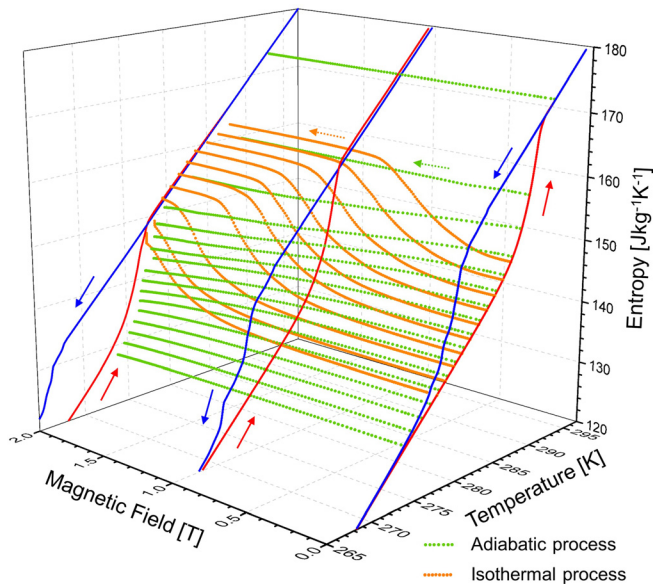


FIG. 3. Three dimensional plot of the  $S(T, H)$  diagram. The red and blue curves indicate the entropy in 0, 1, and 2 T under heating and cooling. The green dotted lines are the transition paths of the first field application under adiabatic conditions starting at different temperatures. The orange dotted curves show the paths under isothermal conditions starting at different temperatures.

is reached at about 0.8 T. For higher fields, the  $\Delta S_T$  remains unchanged at a constant level. At lower starting temperatures, higher field changes are required to complete the transformation and therefore, the plateau becomes smaller.

The adiabatic processes (green dotted lines) were initiated at comparable temperatures. Due to the inverse magnetocaloric effect, the sample temperature decreases when applying a magnetic field. Therefore, a horizontal path through the  $S(T, H)$  diagram is described. In the maximum magnetic field, the dotted lines end in the proximity of the 2 T entropy curve under heating. A video of the rotating 3D diagram from which the specific path can be traced much easier is provided in the [supplementary material](#).

In Fig. 4, the paths of minor hysteresis loops are illustrated in a magnified section of the 3D  $S(T, H)$  diagram discussed before (compared with Fig. 3). The four horizontal loops (green) were measured under adiabatic conditions and the five vertical loops (orange) correspond to isothermal measurements. Their enclosed areas are all filled half-transparent in order to visualize the intersections of the loops. Also for this 3D illustration with minor loops, a video of the rotating  $S(T, H)$  diagram can be found in the [supplementary material](#). It can be seen that the magnetizing branches (segments in the background) meet at certain points. For the demagnetizing branch (curves in the foreground), however, this is not the case. The adiabatic loops pass through the mid regions of the three isothermal loops in the middle. This raises the question what is the difference between the adiabatic process under cycling compared to the isothermal one.

In order to answer this question, we scaled the  $\Delta T_{ad}$  and  $\Delta S_T$  curves in the way that they lie on top of each other. This approach is an extension of previous works.<sup>21,22</sup> The fraction of the austenite is considered to be the ratio of the actual value of the magnetocaloric effect divided by the  $\Delta T_{ad}$  or

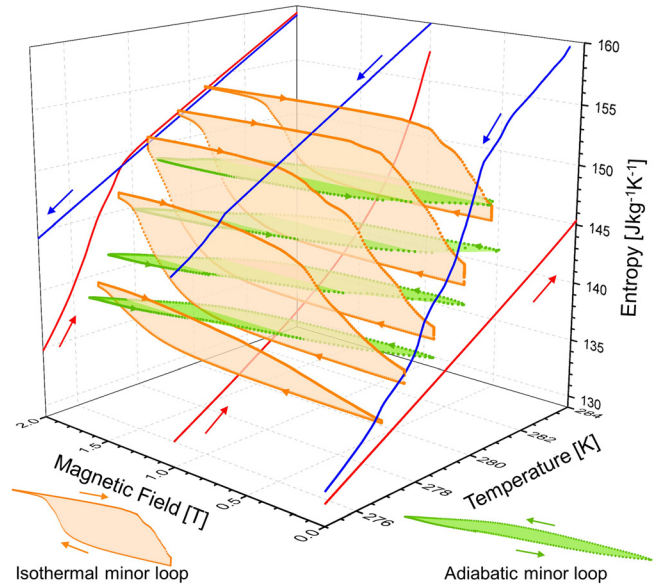


FIG. 4. Magnified portion of the 3D  $S(T, H)$  diagram showing the transformation paths of selected minor loops of hysteresis under isothermal (orange) and adiabatic (green) conditions.

$\Delta S_T$  of the complete transition, respectively. Furthermore, an effective temperature is introduced

$$T_{\text{eff}} = \begin{cases} T_{\text{start}} - \frac{dT_t}{dH} \cdot H, & \text{isothermal} \\ T_{\text{start}} + \Delta T_{ad} - \frac{dT_t}{dH} \cdot H, & \text{adiabatic} \end{cases}$$

with  $T_{\text{start}}$  at which the experiment was initiated and  $\frac{dT_t}{dH}$  being the shift of the transition temperature due to the magnetic field (see Fig. 1). The results for two adiabatic and isothermal minor loops are compared in Fig. 5. In this scaled form, now the curves are actually very similar showing the same characteristics. But there is still one essential difference. In an isothermal process, the Gibbs free energies of austenite and martensite shift when a magnetic field is applied and consequently, the transition temperature changes. In the adiabatic process, this is the case too but in addition the sample temperature changes as well. For this trivial reason, the minor loops for a given magnetic field change are smaller

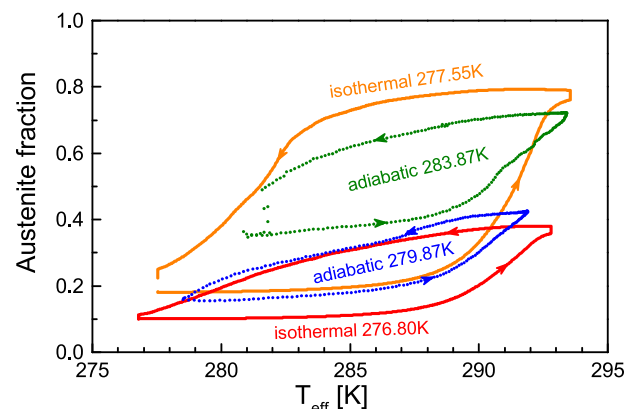


FIG. 5. Scaled minor loops of hysteresis under adiabatic (green and blue) and isothermal conditions (orange and red) with their respective starting temperatures.



under adiabatic conditions or in other words, a larger field would be required in order to enter the same loop as in the isothermal case. Since all experiments were started at zero field (see Fig. 3), the magnetizing branches are still close to the major hysteresis loop and consequently the paths meet at specific points. The actual minor loop is defined by magnetic field reversal. In a simple picture, the significant temperature change of the material itself is hindering the progress of the phase transformation during the field application. The shift of the transition temperature created by the magnetic field change needs to overcome the  $\Delta T_{\text{ad}}$  first. In the same magnetic field change of 2 T, less material is transformed back and forth in the adiabatic process due to the corresponding temperature change of the sample. Therefore, the hysteresis loop under cycling is smaller than in the isothermal case. Those aspects should hold true for other materials undergoing the minor loop behavior as well and therefore, special measurement protocols need to be applied in order to properly determine their magnetocaloric effects under cycling.

In this work, we studied the reversible magnetocaloric effect in minor hysteresis loops. It could be demonstrated that the reversibility in Heusler alloys is significantly larger as predicted by the  $S(T, H)$  diagram implying that it cannot be estimated by standard isofield measurements alone. Our results show that the transformation path of the minor loop depends on whether adiabatic or isothermal conditions are present. By using a scaling routine, we were able to collapse those minor loops. This approach revealed that the transformation mechanism in minor hysteresis loops of the martensitic transition is equivalent for adiabatic and isothermal processes although the  $\Delta T_{\text{ad}}$  reduces the width of the adiabatic loops. Despite this fact, it is interesting that the resulting area of the entropy diagram in which a reversible magnetocaloric effect is possible (see Fig. 2) is actually the same. This implies that it is feasible to estimate the cyclic isothermal entropy change  $\Delta S_T$  based on  $\Delta T_{\text{ad}}$  data under cycling and vice versa. Furthermore, we showed that the optimal condition for a minor loop is fulfilled when similar amounts of martensite and austenite coexist in the material. In this case, the energy-intensive nucleation process can be suppressed most effectively in favor of the much easier phase boundary motion. We conclude that under optimal conditions of similar fractions of coexisting phases in the material, minor loops give rise to an enhanced reversibility. This is an important result that should open new opportunities in implementing Heusler materials in actual solid-state cooling devices.

See [supplementary material](#) for two animated videos of the rotating 3D  $S(T, H)$  diagrams of major and minor hysteresis loops.

This work was supported by DFG (Grant No. SPP 1599) and CICYT (Spain) project MAT2016-75823-R.

- <sup>1</sup>A. Smith, C. R. Bahl, R. Bjørk, K. Engelbrecht, K. K. Nielsen, and N. Pryds, *Adv. Eng. Mater.* **2**, 1288 (2012).
- <sup>2</sup>X. Moya, S. Kar-Narayan, and N. D. Mathur, *Nat. Mater.* **13**, 439 (2014).
- <sup>3</sup>I. Takeuchi and K. Sandeman, *Phys. Today* **68**(12), 48 (2015).
- <sup>4</sup>B. Emre, S. Yüce, E. Stern-Taulats, A. Planes, S. Fabbri, F. Albertini, and L. Mañosa, *J. Appl. Phys.* **113**, 213905 (2013).
- <sup>5</sup>V. V. Khovaylo, K. P. Skokov, O. Gutfleisch, H. Miki, R. Kainuma, and T. Kanomata, *Appl. Phys. Lett.* **97**, 052503 (2010).
- <sup>6</sup>S. Fähler, U. K. Röbber, O. Kastner, J. Eckert, G. Eggeler, H. Emmerich, P. Entel, S. Müller, E. Quandt, and K. Albe, *Adv. Eng. Mater.* **14**, 10 (2012).
- <sup>7</sup>V. Srivastava, X. Chen, and R. D. James, *Appl. Phys. Lett.* **97**, 014101 (2010).
- <sup>8</sup>T. Gottschall, K. P. Skokov, B. Frincu, and O. Gutfleisch, *Appl. Phys. Lett.* **106**, 021901 (2015).
- <sup>9</sup>K. P. Skokov, V. V. Khovaylo, K.-H. Müller, J. D. Moore, J. Liu, and O. Gutfleisch, *J. Appl. Phys.* **111**, 07A910 (2012).
- <sup>10</sup>K. Skokov, K.-H. Müller, J. Moore, J. Liu, A. Karpenkov, M. Krautz, and O. Gutfleisch, *J. Alloys Compd.* **552**, 310 (2013).
- <sup>11</sup>E. Stern-Taulats, P. O. Castillo-Villa, L. Mañosa, C. Frontera, S. Pramanick, S. Majumdar, and A. Planes, *J. Appl. Phys.* **115**, 173907 (2014).
- <sup>12</sup>T. Kihara, X. Xu, W. Ito, R. Kainuma, and M. Tokunaga, *Phys. Rev. B* **90**, 214409 (2014).
- <sup>13</sup>A. Planes, J. L. Macqueron, and J. Ortín, *Philos. Mag. Lett.* **57**, 291 (1988).
- <sup>14</sup>V. Basso, C. P. Sasso, K. P. Skokov, O. Gutfleisch, and V. V. Khovaylo, *Phys. Rev. B* **85**, 014430 (2012).
- <sup>15</sup>T. Gottschall, K. P. Skokov, D. Benke, M. E. Gruner, and O. Gutfleisch, *Phys. Rev. B* **93**, 184431 (2016).
- <sup>16</sup>E. Stern-Taulats, A. Gràcia-Condal, A. Planes, P. Lloveras, M. Barrio, J.-L. Tamarit, S. Pramanick, S. Majumdar, and L. Mañosa, *Appl. Phys. Lett.* **107**, 152409 (2015).
- <sup>17</sup>T. Gottschall, K. P. Skokov, F. Scheibel, M. Acet, M. G. Zavareh, Y. Skourski, J. Wosnitza, M. Farle, and O. Gutfleisch, *Phys. Rev. Appl.* **5**, 024013 (2016).
- <sup>18</sup>O. Gutfleisch, T. Gottschall, M. Fries, D. Benke, I. Radulov, K. P. Skokov, H. Wende, M. Gruner, M. Acet, P. Entel, and M. Farle, *Phil. Trans. R. Soc., A* **374**, 20150308 (2016).
- <sup>19</sup>T. Gottschall, K. P. Skokov, R. Burriel, and O. Gutfleisch, *Acta Mater.* **107**, 1 (2016).
- <sup>20</sup>T. Gottschall, "On the magnetocaloric properties of Heusler compounds: Reversible, time- and size-dependent effects of the martensitic phase transition," Ph.D. thesis, TU Darmstadt, 2016.
- <sup>21</sup>J. Liu, T. Gottschall, K. P. Skokov, J. D. Moore, and O. Gutfleisch, *Nat. Mater.* **11**, 620 (2012).
- <sup>22</sup>J. S. Blázquez, V. Franco, A. Conde, T. Gottschall, K. P. Skokov, and O. Gutfleisch, *Appl. Phys. Lett.* **109**, 122410 (2016).